



Constraints on Compact Dark Matter with Fast Radio Burst Observations

Kai Liao¹, S.-B. Zhang^{2,3,4,5}, Zhengxiang Li⁶, and He Gao⁶¹ School of Science, Wuhan University of Technology, Wuhan 430070, People's Republic of China; liaokai@whut.edu.cn² Purple Mountain Observatory, Chinese Academy of Sciences, Nanjing 210023, People's Republic of China³ University of Chinese Academy of Sciences, Beijing 100049, People's Republic of China⁴ CSIRO Astronomy and Space Science, P.O. Box 76, Epping, NSW 1710, Australia⁵ International Centre for Radio Astronomy Research, University of Western Australia, Crawley, WA 6009, Australia⁶ Department of Astronomy, Beijing Normal University, Beijing 100875, People's Republic of China

Received 2020 March 30; revised 2020 May 21; accepted 2020 May 26; published 2020 June 10

Abstract

Fast radio bursts (FRBs) are bright radio transients with millisecond duration at cosmological distances. Since compact dark matter/objects (COs) could act as lenses and cause splitting of these kinds of very short duration signals, Muñoz et al. have proposed a novel method to probe COs with lensing of FRBs. In this Letter, we for the first time apply this method to real data and give constraints of the nature of COs with currently available FRB observations. We emphasize that the information from dynamic spectra of FRBs is quite necessary for identifying any lensed signals and find no echoes in the existing data. The null search gives a constraint comparable to that from galactic wide binaries, though the methods of redshift inference from the dispersion measure would impact a little. Furthermore, we make an improved forecast based on the distributions of real data for the ongoing and upcoming telescopes. Finally, we discuss the situation where one or more lensed signals will be detected. In such a case, the parameter space of COs can be pinned down very well since the lens mass can be directly determined through the observed flux ratio and time delay between split images.

Unified Astronomy Thesaurus concepts: [Gravitational lensing \(670\)](#); [Dark matter \(353\)](#)

1. Introduction

A wide range of galactic and cosmological observations has verified the existence of dark matter, which contributes a considerable part of the total energy density in the universe. The cold dark matter model has successfully explained the observed large-scale structure. However, we still know little about the constituent of dark matter on smaller scales and some issues exist in this standard model. For example, according to the simulation, galaxies like the Milky Way should have thousands of dark matter subhalos surviving from the tide stripping process and appearing in the form of satellite dwarf galaxies, whereas only ~ 10 such dwarfs have been observed in our galaxy and the Andromeda M31 galaxy (Drlica-Wagner et al. 2015). Furthermore, one may conjecture that dark matter (or part of it) consists of compact objects (COs), such as the massive compact halo objects (Mediavilla et al. 2009; Pooley et al. 2009; Wyrzykowski et al. 2011; Monroy-Rodríguez & Allen 2014), primordial black holes (PBHs; Carr & Hawking 1974; Carr 1975), axion miniclusters (Hardy 2017) and compact mini halos (Ricotti & Gould 2009). For convenience, hereafter we take all of them as compact dark matter/objects (COs). Some theoretical analysis allows the mass of COs to be as light as $10^{-7}M_{\odot}$ and as heavy as the first stars $\sim 10^3M_{\odot}$ (Griest 1991).

Probing COs through astronomical observation is therefore crucial to discriminate models and deepen our understanding of the nature of dark matter. Efforts have been devoted with various approaches and some progress has been made in constraining the CO fraction in dark matter f_{CO} and the mass

M_{CO} . While large mass ($\geq 100M_{\odot}$) COs can perturb the wide stellar binaries (Quinn et al. 2009), the microlensing of stars can constrain the COs in the Milky Way with low mass ($\leq 10M_{\odot}$) (Tisserand 2007; Wyrzykowski et al. 2011; Calchi Novati et al. 2013; Udalski et al. 2015; Niikura et al. 2017). By observing the lack of radiation as a result of accretion, one could also give a constraint for large-mass COs with the cosmic microwave background (Ali-Haïmoud & Kamionkowski 2017). Other methods include millilensing of quasars (Wilkinson et al. 2001), lensing of supernovae (Benton Metcalf & Silk 2007), ultra-faint dwarf galaxies (Brandt 2016), and caustic crossing (Oguri et al. 2018). Generally speaking, no robust evidence of COs has been found for $f_{\text{CO}} > 0.1$ in a wide mass range.

The mass range $10\text{--}100M_{\odot}$ has been poorly constrained and attracted most of the attention especially after the gravitational waves (GWs) from binary black holes were directly detected by LIGO/VIRGO (Abbott et al. 2016). The black hole masses are within such a window, which suggests they could be the PBH dark matter (Bird et al. 2016; Sasaki et al. 2016). However, current constraints are too weak (Ricotti et al. 2008; Oguri et al. 2018). More robust and independent evidence is needed to verify such conjecture. Recently, lensing of transients like GWs (Jung & Shin 2019; Liao et al. 2020), gamma-ray bursts (GRBs; Ji et al. 2018), and fast radio bursts (FRBs; Muñoz et al. 2016) were proposed to be very promising in constraining COs. The imprints of COs as lenses correspond to the distorted waveforms of GWs, the autocorrelation in GRB light curves and the echoes of FRB signals.

Remarkably, the FRB method should be the simplest and cleanest even though we do not yet understand the formation mechanism of FRB. FRBs are bright pulses of emission at radio frequencies, most of which have durations of order milliseconds or less (Lorimer et al. 2007; Thornton et al. 2013). The short duration and large brightness make them emit coherently in nature. Most FRBs seem to be one-off, but a few are

repeaters manifesting a longer-lived central engine. Recent studies showed it is possible that a large fraction (or even all) of the FRBs are repeaters, and we just happen to catch one of their bursts (Ravi 2019; Fonseca et al. 2020; Muñoz et al. 2020). While the current event rate is limited by the small fields of view of current radio telescopes, FRB events are supposed to be quite often on the full sky ($\sim 10^4 \text{ day}^{-1}$) (Thornton et al. 2013; Champion et al. 2016). The ongoing wide-field surveys like APERTIF, UTMOST, HIRAX, and CHIME will monitor a considerable fraction of the sky, giving thousands of detections per year. If part of the dark matter consists of COs, there must be a chance that an FRB is within the Einstein radius of a CO, appearing split signals with flux ratio and time delay. Therefore, detections of such lensed signals could statistically infer the fraction and mass of COs in turn (Muñoz et al. 2016). In principle, lensing of FRBs can effectively detect the mass range down to 20–100 M_\odot that gives typical time delays comparable to the intrinsic duration of the signal. Realistic constraints depend on the event number and distributions of signal durations and redshifts. Shorter durations, higher redshifts, and larger event number would give more stringent constraints.

The detected FRB events are timely included in the public catalog⁷ (Petroff et al. 2016). The newest event number is ~ 110 , which gives a statistical sample. We use these data to give a first constraint on COs and discuss more details about identifying the lensed signals in this work. Besides, we also make corrections to the forecast and discuss how we will deal with the detected lensed FRBs. This Letter is organized as follows: in Section 2, we introduce the theory on FRB lensing; in Section 3, we discuss how to identify the lensed signals and apply our method to the existing data, giving the constraints; the forecast and lens mass estimation are shown in Section 4; finally, we summarize and provide discussions in Section 5.1

2. Lensing of Fast Radio Bursts

Gravitational lensing is usually classified by the lens mass scale (equivalently the Einstein radius). For FRB lensing, we suggest that it is more appropriate to take it as strong lensing since we can clearly discriminate the split transient signals, whereas the traditional microlensing limited by the resolution can only observe the overlapped images of constant sources. We take the CO as a point mass whose Einstein radius is given by

$$\theta_E = 2\sqrt{\frac{GM_{\text{CO}}}{c^2 D}} \approx (10^{-6})'' \left(\frac{M_{\text{CO}}}{M_\odot}\right)^{1/2} \left(\frac{D}{\text{Gpc}}\right)^{-1/2}, \quad (1)$$

where the effective lensing distance (called time delay distance as well) $D = D_L D_S / D_{LS}$, which is a combination of three angular diameter distances. Subscripts S and L denote the source and the lens, respectively. Although the spatial resolution in radio observation could reach a very high level, for example, the angular resolution for the FRB 121102 with Very Long Baseline Array is $\sim (10^{-2})''$ (Spitler et al. 2016; Chatterjee et al. 2017; Tendulkar et al. 2017), it is still insufficient to distinguish split images spatially for $M_{\text{CO}} < 10^8 M_\odot$. Therefore, we cannot get the information of COs by measuring θ_E . What one can directly measure is the

time delay between the lensed signals, which is determined by

$$\Delta t = \frac{4GM_{\text{CO}}}{c^3} (1 + z_L) \left[\frac{y}{2} \sqrt{y^2 + 4} + \ln \left(\frac{\sqrt{y^2 + 4} + y}{\sqrt{y^2 + 4} - y} \right) \right], \quad (2)$$

where the dimensionless impact parameter $y = \beta/\theta_E$ stands for the relative source position, z_L is the lens redshift. Obviously, Δt must be larger than the width (w) of the observed signal itself such that the split lensed images can be distinguished as double peaks. This requires y larger than a certain value $y_{\text{min}}(M_{\text{CO}}, z_L, w)$ according to Equation (2).

In addition, the flux/magnification ratio between two images (+, -) can be directly measured as well:

$$R_f \equiv \left| \frac{\mu_+}{\mu_-} \right| = \frac{y^2 + 2 + y\sqrt{y^2 + 4}}{y^2 + 2 - y\sqrt{y^2 + 4}} > 1. \quad (3)$$

To make both lensed images (especially the fainter one) detectable with high enough signal-to-noise ratio (S/N), R_f should not be too large, which requires the impact parameter to be smaller than a certain value $y_{\text{max}} = [(1 + R_{f,\text{max}})/\sqrt{R_{f,\text{max}} - 2}]^{1/2}$. We set the criterion $R_{f,\text{max}} = 5$ following Muñoz et al. (2016).

For a given FRB event at z_S , the lensing optical depth is the probability that the point source is within the perceptible region of any COs along the line of sight:

$$\tau(M_{\text{CO}}, f_{\text{CO}}, z_S, w) = \int_0^{z_S} d\chi(z_L) (1 + z_L)^2 n_{\text{CO}} \sigma(M_{\text{CO}}, z_L, z_S, w), \quad (4)$$

where χ is the comoving distance, n_{CO} is the CO number density, and the cross section is given by

$$\sigma(M_{\text{CO}}, z_L, z_S, w) = \frac{4\pi GM_{\text{CO}} D_L D_{LS}}{c^2 D_S} \times [y_{\text{max}}^2 - y_{\text{min}}^2(M_{\text{CO}}, z_L, w)]. \quad (5)$$

Using the Hubble parameter at lens redshift and the Hubble constant, Equation (4) can be rewritten as:

$$\tau(M_{\text{CO}}, f_{\text{CO}}, z_S, w) = \frac{3}{2} f_{\text{CO}} \Omega_c \int_0^{z_S} dz_L \frac{H_0^2}{H(z_L)} \frac{D_L D_{LS}}{D_S} \times (1 + z_L)^2 [y_{\text{max}}^2 - y_{\text{min}}^2(M_{\text{CO}}, z_L, w)]. \quad (6)$$

We adopt the flat Λ CDM cosmology with total dark matter density $\Omega_c = 0.24$, baryonic matter density $\Omega_b = 0.06$, and Hubble constant $H_0 = 70 \text{ km s}^{-1} \text{ Mpc}^{-1}$. Following other works, we assume a fraction of dark matter is in the form of COs having the same mass M_{CO} , then $f_{\text{CO}} = \Omega_{\text{CO}}/\Omega_c$.

According to the definition, the expected number of lensed FRBs is the sum of the lensing optical depths of all FRBs (for $\tau_i \ll 1$):

$$N_{\text{lensed}}(M_{\text{CO}}, f_{\text{CO}}) = \sum_{i=1}^{N_{\text{total}}} \tau_i(M_{\text{CO}}, f_{\text{CO}}, z_{S,i}, w_i). \quad (7)$$

This equation shows that for the given $(M_{\text{CO}}, f_{\text{CO}})$, it will predict the corresponding number of detectable lensed FRB signals. On the contrary, one can infer $(M_{\text{CO}}, f_{\text{CO}})$ with the number of observed lensed signals. Particularly, if no lensed

⁷ <http://frbcat.org/>

signal is detected, the region in $(M_{\text{CO}}, f_{\text{CO}})$ parameter space that predicts at least one lensed signal should be ruled out, which is the standard analysis pipeline widely used in the literature.

3. Constraints with Current Observations

The number of verified FRBs is rapidly increasing. At the moment of writing this Letter, the reported FRB number is 110. In addition, there are an extra 9 events that are highly considered as the candidates. Although the method only requires the transient nature, most of the candidates do not have the measured widths of the signals and are therefore not used by us in this work. We will introduce how we analyze these data and constrain COs in this section.

3.1. Identifying the Lensed Signals

In Muñoz et al. (2016), the double-peak structure was pointed out to be the feature of a lensed FRB. We have searched such signals in the catalog and find a few existing FRBs that have multiple-peak structure and are likely to be lensed. They are FRB 170827 (Farah et al. 2018), FRB 121002 (Champion et al. 2016), FRB 121102 (repeating) (Hessels et al. 2018), FRB 180814.J0422+73 (repeating) (CHIME/FRB Collaboration et al. 2019), FRB 181112 (Cho et al. 2020), and the very recent FRB 181123 by the Five-hundred-meter Aperture Spherical radio Telescope (Zhu et al. 2020). To identify a lensed signal, we suggest that one should further use the dynamic spectrum information which reflects the intrinsic feature of an FRB. The dynamic spectra of these events are presented in the original papers except for FRB 121002. One can easily tell that FRBs 170827, 121102, 180814.J0422+73, and 181123 are not lensed since the pulses in the dynamic spectra corresponding to different peaks show different structures. It is impossible to fit them using a simple time delay and relative magnification parameters like what lensing requires. Rather than the lensing effect, the multiple peaks of these FRBs must come from the intrinsic substructure of the signals themselves. For example, FRB 181123 has three peaks, but peak 2 only has the higher and peak 3 only has the lower frequency parts compared to peak 1. We plot the dynamic spectrum of FRB 121002 in the upper panel of Figure 1. Lensing of this event was first discussed by Muñoz et al. (2016). The S/N is small such that the dynamic spectrum cannot easily distinguish the two peaks and we cannot compare them. However, the second arrived peak has an intenser pulse than the first one, which is against the prediction of lensing theory. We therefore take it as an unlensed event. We also plot the repeating FRB 121102 in the lower panel for example. It clearly shows the “frequency drift” phenomenon where multiple bursts occur within several milliseconds with decreasing frequencies. At last, it is worth mentioning that the spectrum of FRB 181112 showed two similar pulses with very large flux ratios (Cho et al. 2020). However, the different polarization details and the impossibility of wave effects indicate the peaks should be intrinsic (Cho et al. 2020).

Therefore, we emphasize that it is important to use more information like the dynamic spectra or polarization properties to identify any lensed signals such that the degeneracy between intrinsic substructure and lensing can be broken. A lensed FRB should appear in dynamic spectrum as two pulses with the same shape and only different from each other by flux magnification and time delay (the fainter one comes later as

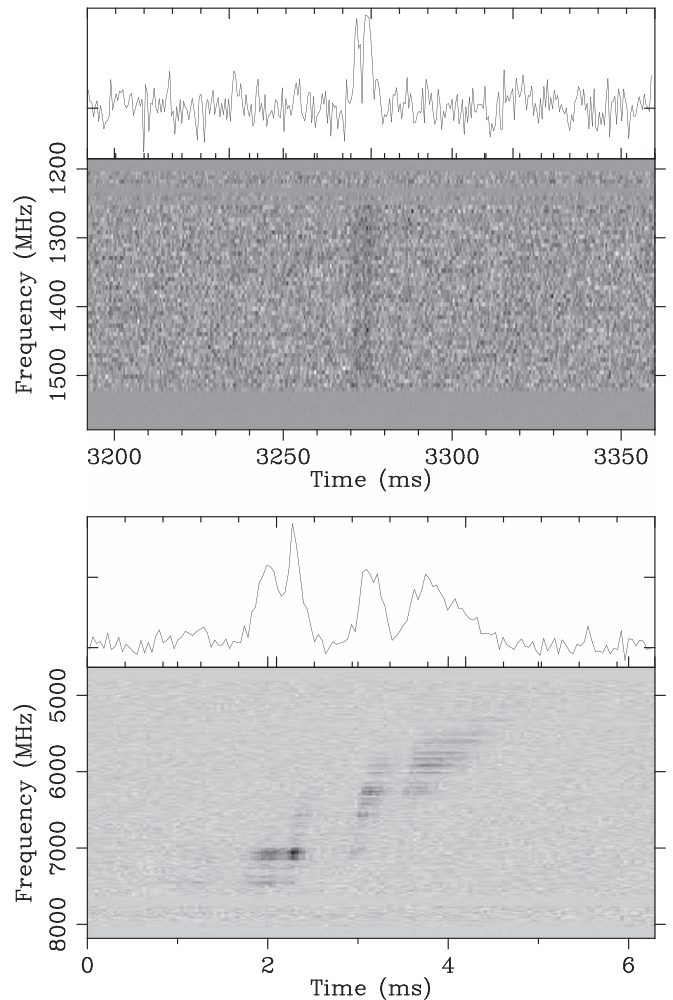


Figure 1. Dynamic spectra of FRB 121002 and a multiple-peak burst of FRB 121102 plotted using the raw data from <https://data-portal.hpc.swin.edu.au/dataset> and <http://seti.berkeley.edu/frb121102>, respectively.

the echo). We have carefully examined the dynamic spectra of the 110 FRBs with their original papers or the raw data on the FRB website, especially those who have multiple peaks. No strong evidence of a lensing signal was found, which can shed light on the properties of lenses.

3.2. Results

The radio pulse from FRB experienced a frequency-dependent delayed time through the ionized interstellar medium, quantified by a dispersion measure (DM), which is proportional to the number of electrons along the line of sight. If we know the ionized history of the universe, we can infer the distances/redshifts with the directly measured DMs. The observed DM of an FRB can be decomposed into

$$\text{DM} = \text{DM}_{\text{MW}} + \text{DM}_{\text{E}}, \quad (8)$$

where

$$\text{DM}_{\text{E}} = \text{DM}_{\text{IGM}} + \frac{\text{DM}_{\text{host}} + \text{DM}_{\text{src}}}{1 + z} \quad (9)$$

is the external DM contribution outside the Milky Way galaxy, and DM_{host} and DM_{src} are from FRB host galaxy and source environment, respectively. The biggest issue in this manner is

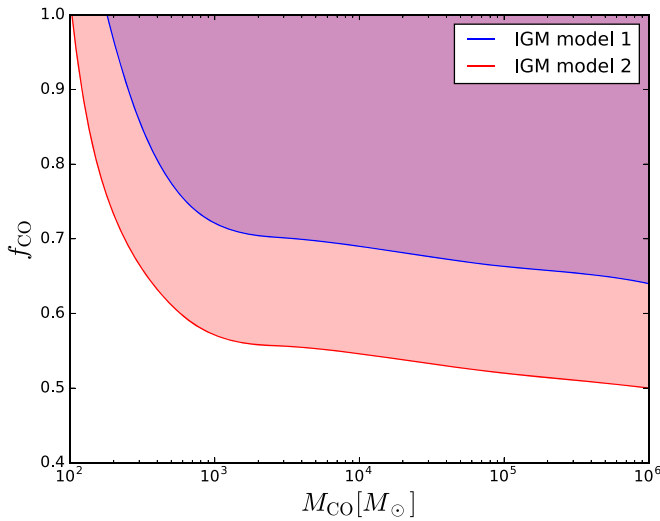


Figure 2. Constraints on the CO fraction and mass based on the fact that no lensed signal has been found in current data. The shaded regions are ruled out. The limits are at the 68% confidence level (1σ) and there are no limits within 2σ .

that we do not have much information on the host galaxy and source environment, except for those who can be localized (Li et al. 2020). The current viewpoint is that the average $DM_{\text{host}} + DM_{\text{src}}$ could span from several tens to $\sim 200 \text{ pc cm}^{-3}$. To make a robust conclusion, we adopt the maximum value 200 pc cm^{-3} , equivalently the minimum inference of z for all host galaxies. For the galactic DM contribution DM_{MW} , we use the NE2001 galactic electron density model (Cordes & Lazio 2002). We adopt two intergalactic medium (IGM) models of inferring redshifts from the rest of the dispersion measure DM_{IGM} . In model 1, we follow the original work by Petroff et al. (2016), where the fraction of baryon mass in the IGM f_{IGM} was supposed to be unity ($f_{\text{IGM}} = 1.0$) and the He ionization history was not taken into consideration, approximately $DM_{\text{IGM}} \sim 1200z \text{ pc cm}^{-3}$ (Ioka 2003). In model 2, the $DM_{\text{IGM}}-z$ relation is given by Deng & Zhang (2014), approximately $DM_{\text{IGM}} \sim 855z \text{ pc cm}^{-3}$ (Zhang 2018), with the consideration of He ionization history and $f_{\text{IGM}} = 0.83$. With the current five localized FRBs, model 2 seems to be more favored (Li et al. 2020).

We follow the standard operating procedure in the literature for studying the nature of COs. For each $(M_{\text{CO}}, f_{\text{CO}})$ point in Figure 2, it corresponds to an expected number of lensed FRB signals according to Equation (7). Since no lensed signal has been found in the current data, the shaded regions in the $(M_{\text{CO}}, f_{\text{CO}})$ parameter space that predict at least one detectable lensed signal should be ruled out at a 68% confidence level (1σ). In the case of IGM model 2, the mass can be tested down to $\sim 100M_{\odot}$ and f_{CO} is gradually constrained to $\sim 0.5-0.6$ for large mass. While in the case of IGM model 1, the constraints are weaker since it gives smaller redshifts. Our results are comparable to that from wide binaries (Quinn et al. 2009). Although current constraints are relatively weak, especially for small masses, we have proved the feasibility of this method. For thousands of events detected in the near future, we will give a much better constraint, especially for small masses ($< 100M_{\odot}$).

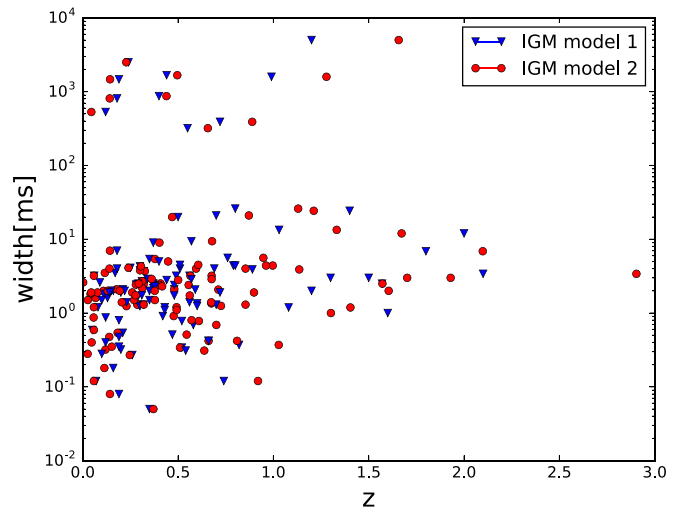


Figure 3. Two-dimensional distribution of widths and inferred redshifts with two methods. We note that a width desert between 30 and 300 ms exists in current data.

4. Forecast

In this section, we use the realistic distributions of the data to make an improved forecast. Furthermore, we discuss how COs can be constrained with detected lensed signals.

4.1. A Null Search Case

In Muñoz et al. (2016), to calculate the integrated lensing probability, the optical depth for lensing of a single burst had to be convolved with the redshift distribution of FRBs. They assumed FRBs either have a constant comoving number density or a scenario where FRBs follow the star formation history. Since we know little about the FRB origin and the DM contribution from host galaxies, there is no reason to make any assumptions for redshift distribution of FRBs. For example, if the progenitors of FRBs are binary stars, then a delay time distribution relative to the star formation rate exists. The direct and more robust way is to understand FRB redshifts from the detected signals themselves. Furthermore, they assumed a constant width of FRB to be 0.3, 1, and 3 ms, respectively, which is not realistic. We make a forecast based on the real distribution of the data. The two-dimensional distribution of widths and redshifts is plotted in Figure 3. The widths are observed ones, rather than the intrinsic. The data are from the FRB website <http://frbcat.org/>, which provides the observed (inferred as well) parameters of each verified signal. The redshifts are inferred from the dispersion measure with two IGM models. The generated events for forecasting follow the 2D distribution in Figure 3, i.e., the simulation follows the observed data themselves. The number 10^4 we assume in this work do not rely on certain surveys. The data from all the telescopes could be used in the analysis. The number is chosen such that we can compare our results with Muñoz et al. (2016). Furthermore, 10^4 FRBs per year is promising for CHIME-like telescopes. The improved forecast is shown in Figure 4. The critical curves are similar to those in Muñoz et al. (2016); however, they are less steep for the small-mass end determined by some very small widths in the catalog, while the decreasing trend persists to large mass due to some very large widths. In addition, we also consider 10^3 events for either the very near future or a pessimistic scenario.

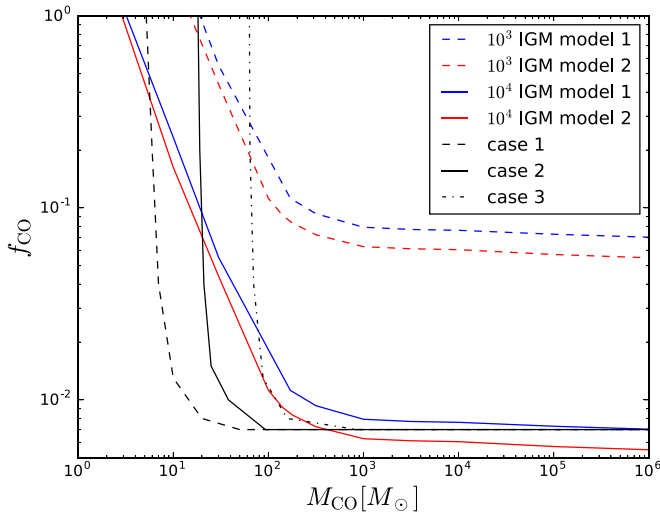


Figure 4. Forecast based on the realistic distributions of the data. The critical lines (red and blue) correspond to the cases that one lensed signal is expected to be detected. We also show the results by Muñoz et al. (2016) for comparison, where the event number is 10^4 , the constant signal widths are 0.3, 1, and 3 ms in case 1, 2, and 3, respectively.

4.2. Constraints from Lensed Signals

We discuss the case in which at least one lensed signal will be verified. Once a lensed FRB signal can be detected, we can estimate the lens mass from the measured time delay and flux ratio. The source position can be determined from the flux ratio, then the redshifted lens mass can be determined from the time delay. Compared to the uncertainties in the measured time delay and flux ratio, the uncertainty of lens redshift dominates. The typical value is $\sigma_{z_L} \sim 0.5$. Nevertheless, it is sufficient for current CO studies. The mass can be pinned down very well on a certain scale. Moreover, if more than one lensed signal is detected, we can even test whether COs consist of the same mass and the theories that give a nonconstant mass function. The intermediate-mass black holes may also be discovered in this way.

To show how this method works, we simulate a typical lensed signal in Figure 5 for example. It uses PSRFITS search mode format covering a frequency range of 1230–1518 MHz of 512 channels. The data are two-bit sampled with a sampling time of $64 \mu\text{s}$. The DMs and widths at a 50% power point of these two pulses are $1000 \text{ cm}^{-3} \text{ pc}$ and 0.5 ms , respectively. The redshift of the FRB $z_S = 1.0$ and the compact dark matter is located at $z_L = 0.5$. The source position relative to the Einstein radius is $y = 0.5$. Assuming a flat ΛCDM model with $\Omega_M = 0.3$ and $H_0 = 70 \text{ km s}^{-1} \text{ Mpc}^{-1}$, the time delay between the two lensed signal can be obtained as $\Delta t = 1.5 \text{ ms}$, the first arrived signal has magnification $|\mu_+| = 1.6$ and the second signal has $|\mu_-| = 0.6$, with flux ratio $R_f = 2.7$. From the dynamic spectrum, one can clearly see two identical pulses except for the time delay and flux ratio differences. If we detect such a signal with Δt and R_f measurements, we can infer the redshifted lens mass $M_z = M_{\text{CO}}(1 + z_L) = 45M_\odot$ based on Equations (2) and (3). However, since z_L cannot be observed, $M_{\text{CO}} = M_z/(1 + z_L)$ inference has the uncertainty from z_L , which should be in $[0, z_S = 1]$, giving $22.5M_\odot < M_{\text{CO}} < 45M_\odot$. Nevertheless, since we have information on M_{CO} , the degeneracy between M_{CO} and f_{CO} can be broken. This would further narrow the allowed regions in

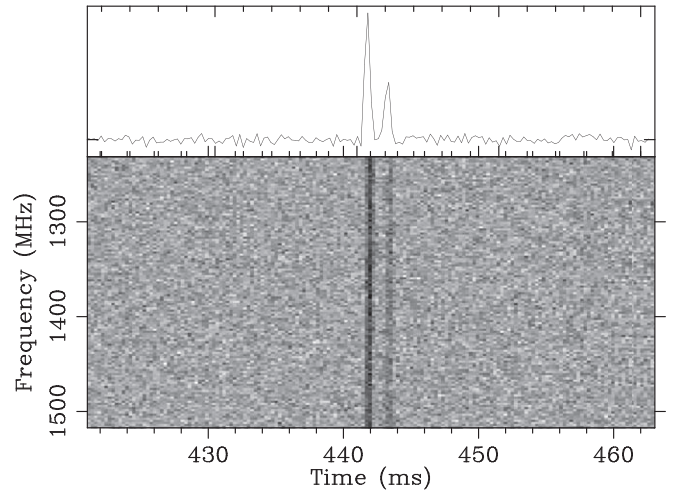


Figure 5. Dynamic spectrum of a simulated lensed signal.

Figures 2 or 4. This idea is very similar to the mass estimation in lensing of gravitational waves (Cao et al. 2014).

5. Summaries and Prospectives

Fast radio bursts are one of the most exciting new mysteries of astrophysics. Beyond how they are created, there is also the prospect of using FRBs to probe the extremes of the universe and the invisible intervening medium. Due to the short duration, cosmological distances and the large event rate, the lensing of FRBs could be a powerful and robust tool to probe the compact dark matter/objects. We have made some progress in this work, summarized as follows.


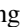

1. For the first time, we use realistic FRB data to give a constraint on the fraction and mass of COs. The constraint results are comparable to that from wide binaries.
2. We make an improved forecast based on the distributions of the existing FRBs for the upcoming CHIME-like experiments.
3. We discuss the importance of using dynamic spectra of FRBs in identifying the lensed signals. It can effectively break the degeneracy between intrinsic structure and lensing imprints.
4. We discuss the situation when a few lensed signals can be detected and find the CO parameter space can be further well determined by lens mass estimation.

For future studies, it is necessary to build up an effective pipeline to identify lensed FRBs, especially for the upcoming large number of FRBs. It is also important to understand the properties of the host galaxies, the ionization history of the universe and its fluctuation in each direction such that the redshift inference can be more accurate. The fast and high spatial resolution program will directly find the host galaxies, thus a large number of redshifts can be measured accurately. More and more events are having polarization measurements, which can be used as an extra criterion for identifying lensed signals, especially for those with similar dynamic spectra, since lensing would not change the polarization. While we were writing this Letter, we noted a very recent work based on analyzing FRB 181112 and 180924 (Sammons et al. 2020). It shows that the burst substructure with high time resolution can

be measured down to $15 \mu\text{s}$ such that much smaller mass scales can be probed, making the FRB method very promising.

We thank the referee for helpful comments and G. Hobbs for his PFITS software package to simulate the lensed signal. K.L. was supported by the National Natural Science Foundation of China (NSFC) No. 11973034. Z.L. was supported by the NSFC No. 11920101003. H.G. was supported by the NSFC Nos. 11722324, 11690024, and 11633001, the Strategic Priority Research Program of the Chinese Academy of Sciences No. XDB23040100, and the Fundamental Research Funds for the Central Universities. S.B.Z. was supported by the NSFC No. 11725314.

ORCID iDs

Kai Liao  <https://orcid.org/0000-0002-4359-5994>
 Zhengxiang Li  <https://orcid.org/0000-0002-8492-4408>
 He Gao  <https://orcid.org/0000-0002-3100-6558>

References

- Abbott, B. P., Abbott, R., Abbott, T. D., et al. 2016, *PhRvL*, **116**, 061102
 Ali-Haïmoud, Y., & Kamionkowski, M. 2017, *PhRvD*, **95**, 043534
 Benton Metcalf, R., & Silk, J. 2007, *PhRvL*, **98**, 071302
 Bird, S., Cholis, I., Muñoz, J. B., et al. 2016, *PhRvL*, **116**, 201301
 Brandt, T. D. 2016, *ApJL*, **824**, L31
 Calchi Novati, S., Mirzoyan, S., Jetzer, P., & Scarpetta, G. 2013, *MNRAS*, **435**, 1582
 Cao, Z., Li, L.-F., & Wang, Y. 2014, *PhRvD*, **90**, 062003
 Carr, B. J. 1975, *ApJ*, **201**, 1
 Carr, B. J., & Hawking, S. W. 1974, *MNRAS*, **168**, 399
 Champion, D. J., Petroff, E., Krameret, M., et al. 2016, *MNRAS*, **460**, L30
 Chatterjee, S., Law, C. J., Wharton, R. S., et al. 2017, *Natur*, **54**, 58
 CHIME/FRB Collaboration, Amiri, M., Bandura, K., et al. 2019, *Natur*, **566**, 235
 Cho, H., Macquart, J.-P., Shannon, R. M., et al. 2020, *ApJL*, **891**, L38
 Cordes, J. M., & Lazio, T. J. 2002, arXiv:astro-ph/0207156
 Deng, W., & Zhang, B. 2014, *ApJL*, **783**, L35
 Drlica-Wagner, A., Bechtol, K., Rykoff, E. S., et al. 2015, *ApJ*, **813**, 109
 Farah, W., Bailes, M., Jameson, A., et al. 2018, *ATel*, **11675**, 1
 Fonseca, E., Andersen, B. C., & Bhardwaj, M. 2020, *ApJL*, **891**, L6
 Griest, K. 1991, *ApJ*, **366**, 412
 Hardy, E. 2017, *JHEP*, **02**, 046
 Hessels, J. W. T., Spitler, L. G., Seymour, A. D., et al. 2018, *ApJL*, **876**, L23
 Ioka, K. 2003, *ApJL*, **598**, L79
 Ji, L., Kovetz, E. D., & Kamionkowski, M. 2018, *PhRvD*, **98**, 123523
 Jung, S., & Shin, C. S. 2019, *PhRvL*, **122**, 041103
 Li, Z., Gao, H., Wei, J.-J., et al. 2020, *MNRAS*, in press (doi:10.1093/mnras/ slaa070)
 Liao, K., Tian, S., & Ding, X. 2020, *MNRAS*, **495**, 2002
 Lorimer, D. R., Bailes, M., McLaughlin, M. A., Narkevic, D. J., & Crawford, F. 2007, *Sci*, **318**, 777
 Mediavilla, E., Muñoz, J. A., Falco, E., et al. 2009, *ApJ*, **706**, 1451
 Monroy-Rodríguez, M. A., & Allen, C. 2014, *ApJ*, **790**, 159
 Muñoz, J. B., Kovetz, E. D., Dai, L., & Kamionkowski, M. 2016, *PhRvL*, **117**, 091301
 Muñoz, J. B., Ravi, V., & Loeb, A. 2020, *ApJ*, **890**, 162
 Niihara, H., Takada, M., Yasuda, N., et al. 2017, *NatAs*, **3**, 524
 Oguri, M., Diego, J. M., Kaiser, N., Kelly, P. L., & Broadhurst, T. 2018, *PhRvD*, **97**, 023518
 Petroff, E., Barr, E. D., Jameson, A., et al. 2016, *PASA*, **33**, e045
 Pooley, D., Rappaport, S., Blackburne, J., et al. 2009, *ApJ*, **697**, 1892
 Quinn, D. P., Wilkinson, M. I., Irwin, M. J., et al. 2009, *MNRAS*, **396**, 11
 Ravi, V. 2019, *NatAs*, **3**, 928
 Ricotti, M., & Gould, A. 2009, *ApJ*, **707**, 979
 Ricotti, M., Ostriker, J. P., & Mack, K. J. 2008, *ApJ*, **680**, 829
 Sammons, M. W., Macquart, J.-P., Ekers, R. D., et al. 2020, arXiv:2002.12533
 Sasaki, M., Suyama, T., Tanaka, T., & Yokoyama, S. 2016, *PhRvL*, **117**, 061101
 Spitler, L. G., Scholz, P., Hessels, J. W. T., et al. 2016, *Natur*, **531**, 202
 Tendulkar, S. P., Bassa, C. G., Cordes, J. M., et al. 2017, *ApJL*, **834**, L7
 Thornton, D., Stappers, B., Bailes, M., et al. 2013, *Sci*, **341**, 53
 Tisserand, P., Le Guillou, L., Afonso, C., et al. 2007, *A&A*, **469**, 387
 Udalski, A., Szymański, M. K., & Szymański, G. 2015, *AcA*, **65**, 1
 Wilkinson, P. N., Henstock, D. R., Browne, I. W. A., et al. 2001, *PhRvL*, **86**, 584
 Wyrzykowski, L., Skowron, J., Kozłowski, S., et al. 2011, *MNRAS*, **416**, 2949
 Zhang, B. 2018, *ApJL*, **867**, L21
 Zhu, W., Li, D., Luo, R., et al. 2020, *ApJL*, **895**, L6